TUDelft

Delft University of Technology

Techno-economic analysis of PSA separation for hydrogen/natural gas mixtures at hydrogen refuelling stations

Burgers, Iris; Dehdari, Leila; Xiao, Penny; Li, Kevin Gang; Goetheer, Earl; Webley, Paul

Techno-economic analysis of PSA separation for hydrogen/natural gas mixtures at hydrogen refuelling stations

Iris Burgers [a], Leila Dehdari [a], Penny Xiao [a], Kevin Gang Li [a], Earl Goetheer [b], Paul Webley [c,*]

[a] Department of Chemical Engineering, The University of Melbourne, Parkville, Victoria, 3010, Australia
[b] Process and Energy, Delft University of Technology, Delft, Zuid-Holland, 2628 CB, the Netherlands
[c] Department of Chemical Engineering, Monash University, Clayton, Victoria, 3800, Australia

HIGHLIGHTS

- A PSA process produces >99% hydrogen from natural gas/hydrogen containing 10% hydrogen.
- A multi-layered bed effectively removes natural gas impurities.
- A PSA process for a 700 kg H2/day refueller supplied from natural gas/hydrogen produces hydrogen from $12–15/kg.
- The PSA supplied hydrogen is cost competitive with local electrolysis supplied hydrogen.

ARTICLE INFO

ABSTRACT

Logistics of hydrogen is one of the bottlenecks of a hydrogen economy. In this study, a pressure swing adsorption (PSA) system is proposed for the separation of hydrogen from natural gas, co-transported in the natural gas grid. The economic feasibility of hydrogen supplied by a PSA system at a refuelling station is assessed and compared with other alternatives. The adsorbent material is key to the design of a PSA system, which determines the operation performance and cost. It is concluded that a refuelling station with hydrogen supplied by a PSA system is economically feasible. The final hydrogen price including hydrogen supply, compression, storage, and dispensing is compared with two other hydrogen supply methods: on-site electrolysis and tube-trailer transported hydrogen. Currently, PSA supplied hydrogen is a more economical option. On-site electrolysis can become a more economical option in the future with improved cell efficiencies and reduced electricity prices. Tube-trailer transported hydrogen is highly influenced by the distance travelled. The findings of this study will help with more efficient distribution of hydrogen.

© 2022 Hydrogen Energy Publications LLC. Published by Elsevier Ltd. All rights reserved.

Introduction

Global warming is a great threat to the environment and is challenging the world we live in today. Transportation is the third largest contributor to greenhouse gas emissions in Australia [1]; therefore, alternative fuels have to be investigated. Hydrogen is a remarkably clean fuel, which only produces water when used in a fuel cell [2]. It contains an energy yield of 122 kJ/g, which is 2.75 times higher compared to fossil fuels [3,4].

Hydrogen is not naturally found, but can be produced in several ways. Common ways of producing hydrogen are through coal gasification and steam methane reforming (SMR), which both emit CO_2 as by-product. A green alternative way of producing hydrogen is water electrolysis by using renewable energy resources, such as solar and wind energy. Renewable energies have stochastic operating conditions, such that at peak production times more energy is produced than the demand requires. One way of storing this energy is in the form of producing hydrogen through electrolysis. This concept is known as power-to-gas, where hydrogen serves as an energy carrier, and is an efficient way of both storing and transporting energy [5]. The generated hydrogen can be transported to hydrogen refuelling stations for fuelling fuel cell vehicles.

There are different ways in which hydrogen can be transported. Pressurised hydrogen is the easiest method, with typical storage pressures of 250 bar–500 bar for transportation in tube-trailers [6]. Furthermore, the hydrogen can be liquefied, in which hydrogen can be transported at a larger volumetric energy density, compared to pressurised hydrogen. The liquefaction process, which is operated at 21 K, does require a high amount of energy and is therefore very costly [7]. The pressurised or liquefied hydrogen can then be transported by tube-trailer or train to the required destination. Another way of storing and transporting hydrogen is using the existing natural gas pipeline network. The grid offers a large transportation and storage network and can be used by injecting the hydrogen into the natural gas pipelines. At any point in the network the hydrogen can be separated from the natural gas and either used directly as a fuel, for transportation for example, or as a feedstock for industrial applications. The injection of up to 10% of hydrogen by volume in the Australian natural gas pipeline network has been reviewed, and it is concluded that there are no significant safety or risk aspects, neither any significant implications with state legislations [8]. This provides great opportunities to investigate the possibilities of using the natural gas grid for the transportation of hydrogen.

In order to use the hydrogen co-transported in the natural gas pipeline as a fuel for fuel cell cars at a refuelling station, a separation of the hydrogen from the natural gas is required. Fuel cell cars require high purity hydrogen, as impurities can damage the fuel cell membrane. Therefore, the ISO 14687–2 norm is established to set a boundary for the quality of hydrogen. The purity of the hydrogen should be at least 99.97%, with a limit for different impurity components as listed in Table 1 [9]. To achieve this, a gas separation method is required which is capable of obtaining this purity standard.

Table 1 – Purity requirements for hydrogen used in fuel cell cars, according to the ISO 14687-2 standard [9].

Impurity	Amount fraction/μmol mol^{-1}
Helium	300
Nitrogen	100
Argon	100
Water	5
Oxygen	5
Carbon dioxide	2
Total hydrocarbon	2
Formic acid	0.2
Carbon monoxide	0.2
Ammonia	0.1
Total halogenated	0.005
Formaldehyde	0.01
Total sulphur	0.004

There are different existing gas separation technologies available, such as absorption, cryogenic distillation, membrane separation, and adsorption. Gas absorption uses a liquid solvent to purify a gas stream. No selective solvent for hydrogen exists, which makes absorption not suitable for the separation of hydrogen and natural gas. Cryogenic separation is the most costly separation method, as it operates at very low temperatures and high pressures [7]. The gases are separated by distillation as partial condensation of the gases occurs at the operating condition. Membrane separation is a very simple, low cost, and energy efficient process typically used for bulk separation. It is driven by a pressure gradient and therefore produces a low-pressure product [7]. Lastly, gas adsorption is the binding of a gas molecule on a solid surface by forming attractive forces at high pressures. Pressure swing adsorption (PSA) is the most commonly used hydrogen purification method used in industry, which exploits the adsorption of gases on adsorbent material at high partial pressures and regenerate the adsorbent while recovering the adsorbed gases at low partial pressures. PSA is able to produce a hydrogen product with high purity and high recovery [10].

Liemberger et al. [11] studied the separation of hydrogen from natural gas, transported in the natural gas pipeline network, using a hybrid system of a membrane and a PSA system, producing a pure hydrogen stream which is suitable for the use of fuel cell cars. The membrane is used to enrich the hydrogen stream, before it is used as a feed for the 4 bed PSA system. Separate experiments on the membrane separation and PSA separation were conducted. A feed stream of 2–4% hydrogen, 1% CO_2, and methane at 51 bar was enriched to a feed stream of 15–22% hydrogen (v/v) at a pressure of 5–6 bar. A separate adsorption experiment was conducted, in which one bed with activated carbon was used. A feed of 20% hydrogen added with methane resulted in a hydrogen product purity of 98% with a recovery of 55–65%. In a follow up paper, the authors investigated different process designs [12].

However, is it also possible to separate hydrogen from a natural gas mixture in one single process? In this initial study, a single PSA system is designed, which aims at separating hydrogen, co-transported with natural gas in the existing gas grid, at a hydrogen refuelling station such that the hydrogen can be used directly as fuel for fuel cell electric vehicles (FCEVs). First of all, the adsorbent materials are selected,

based on current literature data available. Secondly, a process analysis is performed to evaluate the designed PSA process, using an in-house developed process simulator (MINSA). Third, a techno-economic analysis is performed to investigate the feasibility of hydrogen supplied by a PSA at a refuelling station. Lastly, the proposed design is compared with other hydrogen supply methods, namely on-site electrolysis and tube-trailer transported hydrogen.

Method

Adsorbent selection

The adsorbent material is key in the design of a PSA system, which determines the operation performance, design, and cost. Therefore, an adsorbent screening analysis has been performed based on the single component isotherm data found in literature. Hydrogen is a very small and light gas which does not adsorb significantly on any known material at standard temperature and pressure. Therefore, for this separation, all other gases in the mixture must be adsorbed such that pure hydrogen can leave the top of the bed. It is assumed that the gas mixture is taken from the natural gas pipeline at the feed pressure (20 bar), therefore eliminating the need to compress the input feed.

The main gas component in the natural gas mixture is methane. Activated carbon has a large working capacity for methane, and it is available at low cost. An adsorption isotherm of a typical activated carbon is presented in Fig. 1, showing the adsorption of different gas components in the natural gas mixture [13–16]. Heavy hydrocarbons present in the natural gas mixture adsorb very strongly to activated carbons, shown by the steep initial curve in the isotherm for ethane, butane, and pentane. This implies that the gas components may not desorb at the desorption pressure, causing accumulation in the activated carbon. Since the partial pressures of these hydrocarbons present in the gas mixture are
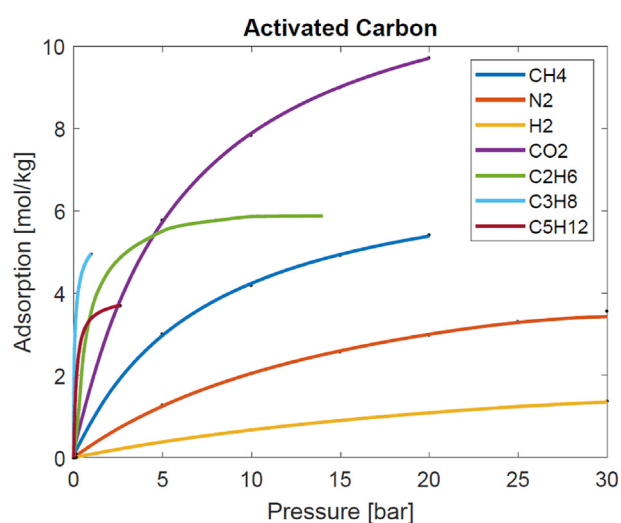
low, the isotherms of these hydrocarbons do not go up until higher pressures as this will not represent the relevant application range. To prevent this, a pre-layer is required, which adsorbs these contaminating gas components (C_2H_6, C_3H_8, C_5H_{12}) before reaching the main layer. This pre-layer material requires a more linear isotherm for the contaminating gases, such that the pre-layer can be regenerated during PSA operation.

It is a common practice to use silica gel as a pre-layer in industrial PSA processes for the adsorption of heavy hydrocarbons and CO_2 [17], because silica gel has a more linear isotherm for all heavy hydrocarbons and CO_2, as represented in Fig. 2 [18]. This will lead to easier regeneration compared to activated carbon. The isotherm provides a good understanding of the adsorption characteristics, and shows desorption is possible within the pressure range of the heavy hydrocarbons and CO_2. Silica gel is also capable of adsorbing mercaptans and any small trace amounts of water present in the gas mixture, which can be harmful to the fuel cell.

Lastly, an adsorbent material is required for the adsorption of nitrogen, as this gas is not adsorbed well on either silica gel or activated carbon. Zeolite LiLSX showed the best working capacity for nitrogen adsorption, and is therefore selected as the post-layer adsorbent material. In Fig. 3 the gas adsorption isotherm of different gas components on zeolite LiLSX is presented [19,20].The adsorption of methane and CO_2 is stronger than for N_2. By using the zeolite as a post-layer in the bed, most methane and CO_2 will already be adsorbed in the activated carbon or silica gel. Therefore, the mole fraction of N_2 will be much higher and thus the selective adsorption of N_2 will be greater, and in that way it will remove the N_2 from the gas mixture.

In summary, a three-layered adsorption column is designed in which each layer adsorbs a different gas or group of gases. As methane is the predominant component of the gas mixture, activated carbon will be the main adsorbent layer. A pre-layer of silica gel is used to adsorb the heavy hydrocarbons, such that accumulation of these gases on the activated carbon is prevented. A post-layer of zeolite LiLSX is

Fig. 1 – **Adsorption isotherms of different gases present in the gas mixture on an activated carbon sample at 289K. Based on literature data from Refs. [13–16].**
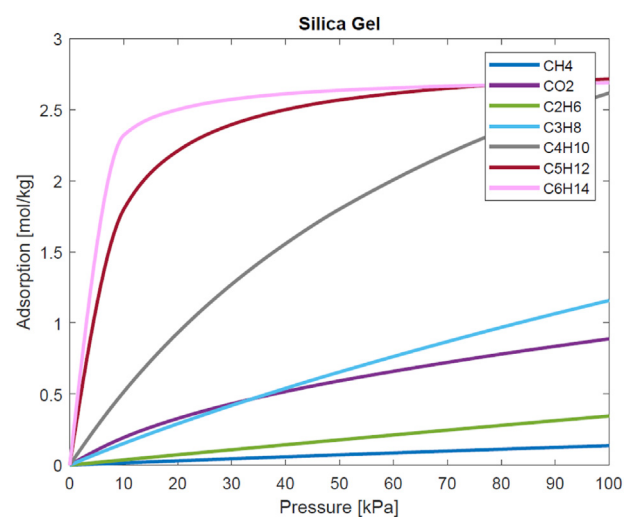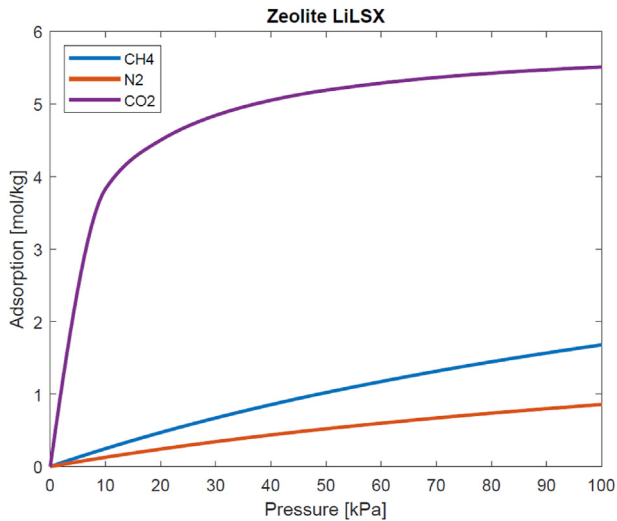

Fig. 2 – **Adsorption isotherms of different gas components on silica gel at 298K. Based on literature data from Ref. [18].**

Fig. 3 – Adsorption isotherms of different gas components on zeolite LiLSX [19,20].

used for the adsorption of the remaining N_2 at the end of the bed.

PSA process design

The designed pressure swing adsorption system consists of 6 beds, each undergoing 12 steps per cycle, which is schematically depicted in Fig. 4. A large number of beds is required to facilitate the pressure equalisation steps, which ensures a high hydrogen recovery. The cycle consists of an adsorption step, four pressure equalisation steps, a blow down step, and a repressurisation step using part of the pure hydrogen product. In the presence of the high purity hydrogen, the remained adsorbed gas components in the void space desorb, providing a cleaner bed at the start of the following adsorption step in the new cycle, resulting in a higher hydrogen purity product without decreasing the recovery. The pressure profile of 1 bed as a function of the cycle time is presented in Fig. 5.
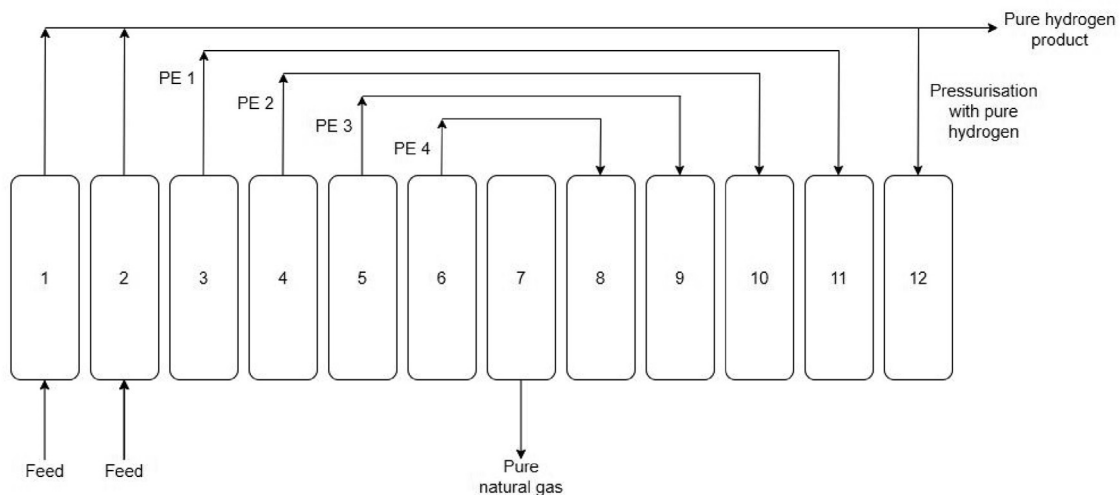
The process analysis evaluates the influence of the silica gel pre-layer for the adsorption of contaminants for the main bed. Three different thicknesses were assessed: 0.1, 0.2, and 0.3 m of silica gel pre-layer. The total height of the column was kept constant at 1.2 m and the zeolite LiLSX post-layer is kept at a fixed thickness of 0.1 m. The goal was to find the optimal pre-layer thickness in the 6 bed 12 step process cycle. In order to perform the process simulations, the inhouse simulator MINSA (Monash Integrated Numerical Simulator for Adsorption) has been used [21,22]. MINSA is a PSA process simulator, which uses the finite volume method to discretise the coupled partial differential equations, for the conservation of mass and energy, in space. A reliable result was assumed when cyclic steady state (CSS) was achieved, which was found to be achieved after more than 1000 cycles. See Supporting Information for more detail.

The simulations were performed for a hydrogen concentration of 10 vol % in the feed gas stream mixed with natural gas. The design parameters used in the simulations were based on a pilot scale PSA design, previously designed and tested by our group at a scale of 100 m^3/h feed gas. The processing conditions are tabulated in Table 2. The pressure is assumed to be 20 bar, which corresponds with connecting the PSA system with the natural gas grid at the secondary main transmission pipeline (typically at pressures between 10 and 70 bar).

The composition of natural gas in the Moomba (NSW, Australia) gas line was used, and listed in Table 3 [8]. This gas line is connected to both New South Wales and South Australia; therefore it is decided that this composition is a good starting point for this study as it has a broad application.

Economic assessment for building a hydrogen refuelling station

A hydrogen refuelling station, where the PSA system supplies the hydrogen, is designed and the economic feasibility is assessed. For this design, a total of 10 vol % hydrogen is assumed in the feed mixture, supplied through the existing pipeline network at a pressure of 20 bar. Since the PSA system

Fig. 4 – Overview of designed PSA system with 6 beds. Four pressure equalisation steps are used to increase the hydrogen recovery, and the purity of the hydrogen is enhanced by the final pressurisation step with the pure hydrogen product.
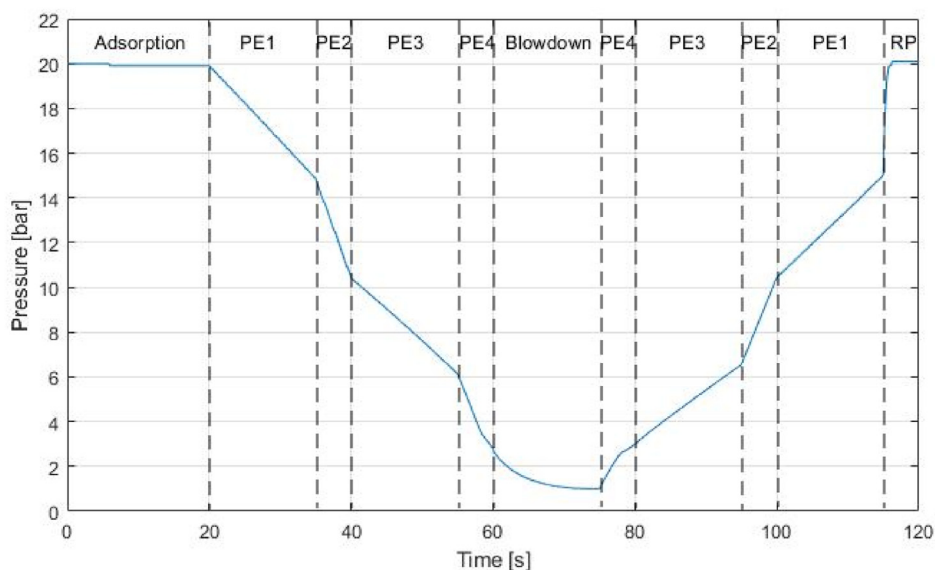
Fig. 5 – Pressure profile of the 6 bed and 12 step PSA system as a function of the cycle time. The adsorption pressure is 20 bar. (PE – pressure equalisation, RP – repressurisation).

operates at 20 bar, it was decided to locate the PSA system near a pipeline delivering the gas at the same pressure, to eliminate the need to pressurise the input gas. The design of the refuelling station will be analysed for the PSA and for the storage, compression, and dispensing design for a medium sized refuelling station, producing 700 kg of hydrogen per day [23]. The storage tank of a fuel cell car is 5 kg of hydrogen at 700 bar, which results in a maximum number of cars refuelling per day of 140.

The compression and storage required at the refuelling station to meet the demand is evaluated using the Hydrogen Refuelling Station Analysis Model (HRSAM) [24]. It is developed to find the optimum size for the compression and storage tanks, while minimizing the refuelling costs. The optimisation can be done for a user set daily hydrogen demand and for two different gaseous hydrogen delivery methods: as compressed gas by tube-trailers or as a pure gas at 20 bar delivered by a pipeline.

This model uses a cascade system, each consisting of 3 tanks of the same size, with a different minimum pressure, representing a low, medium, and high-pressure vessel. When refuelling, hydrogen is first drawn from the low-pressure vessel,

followed by the medium, and then the high-pressure vessel. Furthermore, there is a low-pressure storage which has a capacity of approximately 30% of the daily demand, storing the hydrogen at 20 bar. The compressor supplies hydrogen from the low pressure storage tank to the cascade system to ensure the appropriate pressures in the different tanks is continuously maintained. An additional back up compressor is considered in the design by the HRSAM model as well.

The capital investment costs, such as site preparation, engineering & design, project contingency, etc., are estimated as a percentage of the initial capital investment cost (see Table 12). The operational & maintenance (O&M) cost consist of labour cost ($25.40 per hour [25]), electricity costs (5–25 c/kWh) and maintenance cost (calculated as percentage of capital investment costs), calculated for each operating component (see Supporting Information for more detail).

The PSA process is the fundamental part of the refuelling station which determines the hydrogen production per day. Based on the performed process analysis in this study, for a 10 vol % hydrogen in the input feed, 20 kg of hydrogen can be produced per day. The PSA columns have to be scaled to meet

Table 2 – Processing conditions for simulations performed with MINSA.

Condition	Value	Unit
Adsorbent bed		
Feed pressure	20	bar
Desorption pressure	1	bar
Feed gas H_2 concentration	10	%
Feed time	31	s
Flow rate	100	sm^3/hr
Operating temperature	298	K
Column height	1.2	m
Column inner diameter	0.3	m
Pre-layer thickness	0.1, 0.2, 0.3	m

Table 3 – Gas composition of Moomba gas in New South Wales and South Australia with 10 vol % H_2 [8].

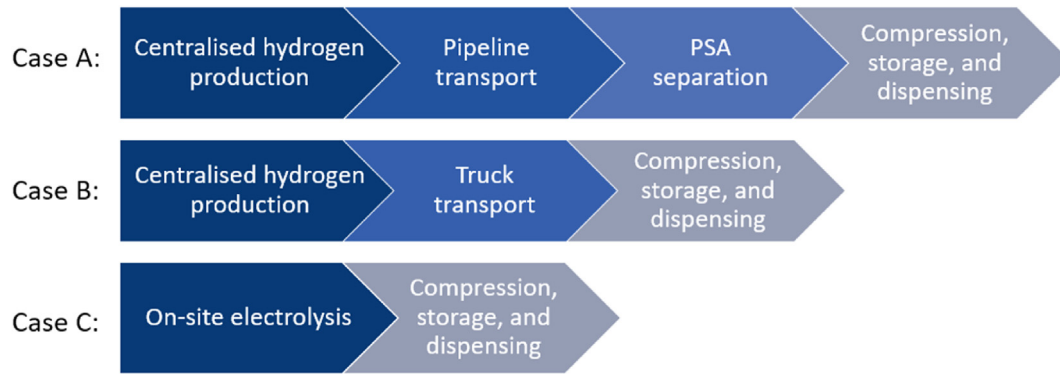| Component	Concentration [mol %]
Methane	86.14
Ethane	2.132
Propane	0.064
i-Butane	0.004
n-Butane	0.007
i-Pentane	0.002
n-Pentane	0.005
n-Hexane	0.014
Nitrogen	1.147
Carbon Dioxide	0.487
Hydrogen	10

Fig. 6 – Overview of the three different hydrogen supply methods considered in the comparison.

the hydrogen demand. The sizing of the PSA is based on by fixing the flowrate and scaling the height and the inner diameter of the adsorption bed, keeping the ratio of the height over the diameter constant. Due to the high operating pressure, a narrow and tall column is more beneficial in order to distribute the pressure evenly and to transfer the heat generated during adsorption (see Table 6 for more details on the scale-up parameters).

A continuous operation of the PSA is assumed, as this results in the smallest columns for the PSA process. The PSA cycle is easily paused and continued; therefore, the operation time of the PSA is controlled by the hydrogen demand. A pressure based system, in which the PSA is switched on as soon as the pressure in the hydrogen storage tank drops below a certain threshold, is utilised. If necessary, the PSA runs 24 h on a day, to meet the hydrogen fuelling demand. If the demand is lower at a given day, the PSA operation is limited to what is required, saving energy for the separation process and for the compression as well.

In the techno-economic analysis, the cost for hydrogen production by PSA and the cost for compression and storage are calculated. A medium sized refuelling station, producing 700 kg of hydrogen per day, is considered. The final cost price of hydrogen is then compared to other possible hydrogen supply methods at a hydrogen refuelling station. An overview of the different cases considered is depicted in Fig. 6. The first case uses a PSA system to separate the pipeline transported hydrogen from the natural gas. The second case assumed centrally produced hydrogen transported by tube-trailer to the station. The last case considers on-site hydrogen production through electrolysis. All methods require on-site compression, storage, and dispensing.

Results and discussion

Process analysis

The simulation results for a 10 vol % hydrogen input feed are presented in Table 4. Fig. 7 shows the gas concentration profiles and the solid loading profiles for the different components in the gas mixture at the end of the adsorption step as a function of the length of the bed.

The results show that a hydrogen product purity of 99.7% is achieved for all pre-layer thicknesses. The larger the pre-layer, the smaller the adsorption of the heavy hydrocarbons in the activated carbon layer (Fig. 7 (ii) and (iv)). The total amount adsorbed on the silica gel layer is relatively low, because the adsorption of the heavy hydrocarbons is less strong on silica gel compared to the adsorption on activated carbon. It is, however, beneficial to have a less strong adsorption of the heavy hydrocarbons in the pre-layer, such that desorption of the gases can be ensured. The adsorption of the heavy hydrocarbons in the final zeolite LiLSX layer is rather strong, (see Fig. 7 (ii) and (iv)). However, the concentration of the heavy hydrocarbons is close to zero at this point in the bed (see Fig. 7 (i) and (iii)), therefore, the total amount of heavy hydrocarbons that will be adsorbed in this layer is limited and will not interfere with the N_2 adsorption in the zeolite layer (see Fig. 7(viii)). It is therefore concluded that, as a result of the pre-layer, the heavy hydrocarbons do not accumulate in the bed and thus the rest of the bed is protected. A further increase in the pre-layer is not considered, as this will reduce the thickness of the main activated carbon layer too much, leaving not enough material to adsorb all the methane.

Table 4 – Overview of the simulation results for a hydrogen input feed of 10 vol %, for a varying silica gel pre-layer thickness. The zeolite LiLSX layer is kept constant at 0.1 m, whereas the activated carbon layer changes proportionally with the silica gel pre-layer, keeping the total height of the column constant.

Pre-layer [m]	Top output [%]		Bottom output [%]		Total hydrogen product output [kg/day]
	H_2 purity	H_2 recovery	CH_4 purity	H_2 concentration	
0.1	99.70	95.72	95.33	0.41	20.74
0.2	99.78	94.98	95.26	0.52	20.58
0.3	99.77	94.06	95.08	0.64	20.38
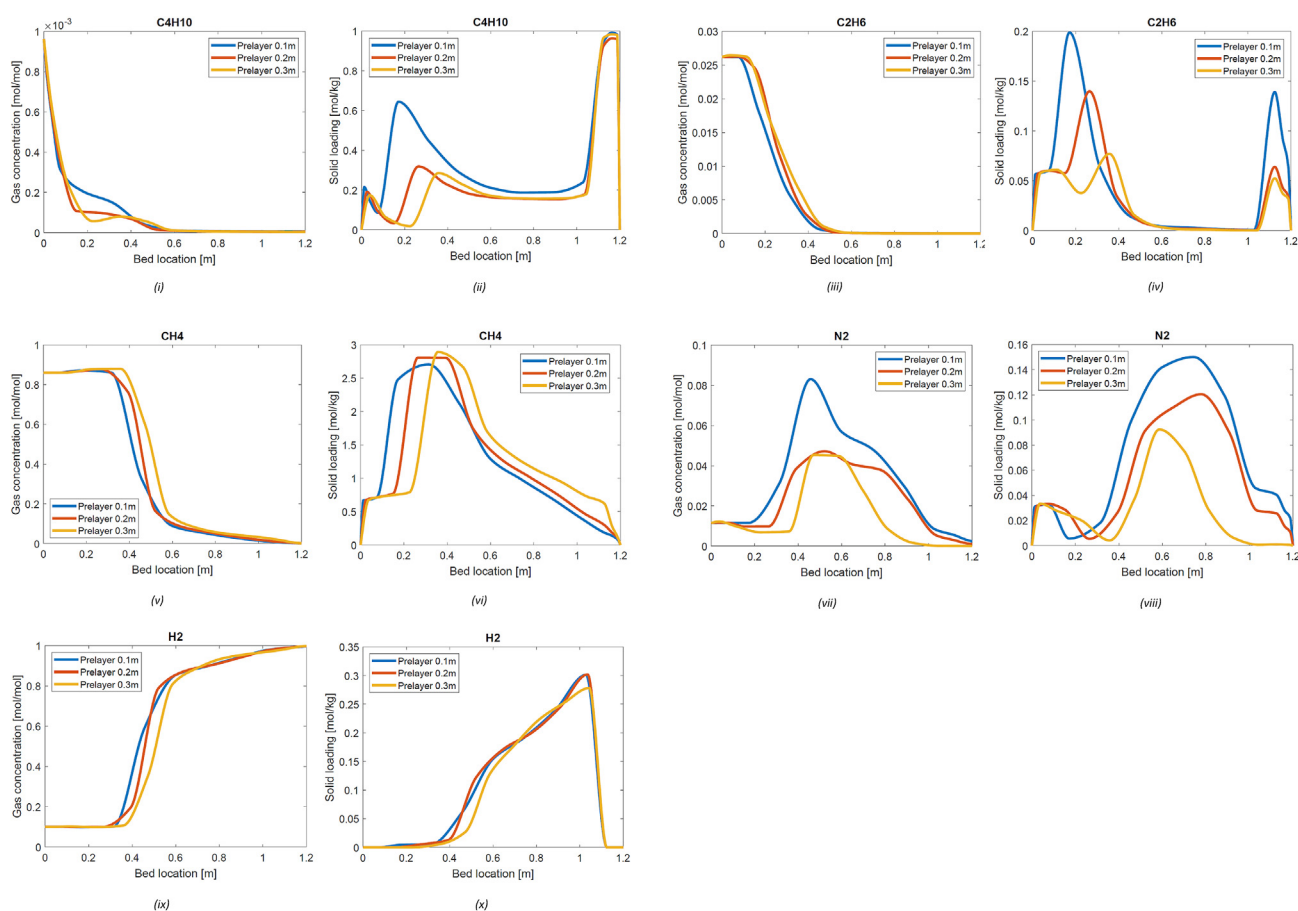
Fig. 7 – Gas concentration and solid loading profiles at the end of the adsorption step for a 10% hydrogen feed input. Figure (i) and (ii) represent the grouped heavy hydrocarbons, figure (iii) and (iv) represent ethane and CO₂ grouped together. Figure (v) and (vi) show the profiles for methane, figure (vii) and (viii) show nitrogen, and lastly figure (ix) and (x) represent hydrogen.

Fig. 7 (v) and (vi) represent the gas concentration and solid loading of methane throughout the bed. A small delay in the adsorption of methane is observed as a result of the increased thickness of the pre-layer. The amount of methane adsorbed in the third scenario, where a pre-layer of 0.3 m is used, is slightly higher near the end of the bed, due to the smaller amount of activated carbon left in the column as the total height was kept constant. For this reason, no simulations are performed in which a longer pre-layer is used, as this will only further reduce the main activated carbon layer.

From Fig. 7 (vii) and (viii), it can be concluded that most of the nitrogen is already adsorbed in the main activated carbon layer. Only a very small concentration of nitrogen is left at the end of the bed, hence the solid loading is reduced as well. Lastly, Fig. 7 (ix) and (x) represent the hydrogen concentration and solid loading as a function of the bed location. This clearly shows the hydrogen concentration increase throughout the column. Only a small amount of hydrogen is adsorbed in the main activated carbon layer.

The hydrogen recovery achieved for all cases is >94% and the methane purity in the bottom product is for all simulations around 95%. The amount of hydrogen in the bottom product is always below 1%. The total amount of hydrogen produced during a full day is around 20 kg of hydrogen with a feed input concentration of 10 vol %. The simulations are optimised for a high hydrogen purity product and a high recovery. In the design of the PSA process, a trade-off must always be made between a high purity and a high recovery. The simulations performed during this study focused on the optimisation of the PSA process for a high purity hydrogen (of >99%) and a high recovery. A high recovery is economically beneficial, however, in this case it means that the purity of the hydrogen achieved does not meet the fuel cell quality requirements (see Table 1). At the end of the separation, small amounts of methane, N_2 and hydrocarbons are present in the H_2 stream which are above the ISO standard [9] (see Fig. 10 in the Supporting Information).

In order to achieve the purity requirements for the fuel cell with the proposed PSA system, different options can be considered. First of all, the purity will increase by decreasing the adsorption time. This, however, does significantly reduce the recovery of the system as well, and therefore an economical trade-off must be made between purity and recovery. Furthermore, an additional purifying unit can be used, such as a simple two bed PSA system, which focuses on the adsorption of the hydrocarbons left in the hydrogen product. The hydrogen product can also be purified by a membrane, either before the hydrogen is fed into the PSA system, as
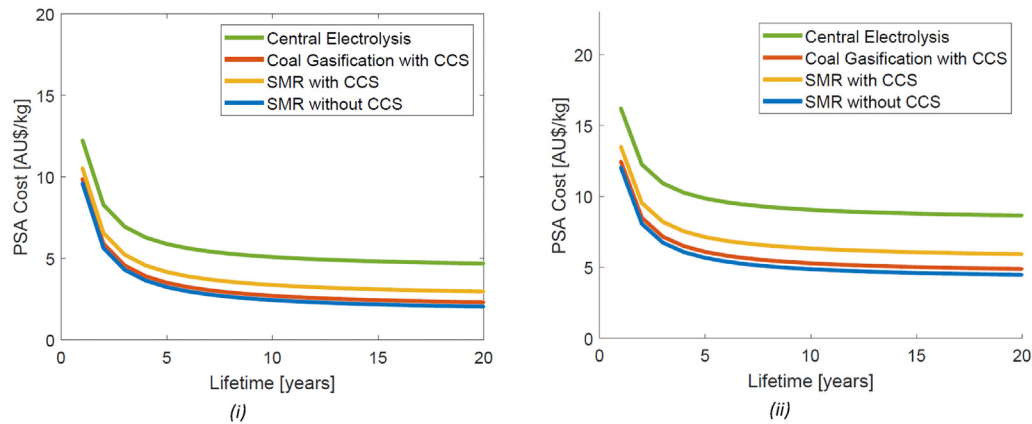
Fig. 8 − Cost PSA system as a function of the lifetime, for different hydrogen production methods. Figure (i) represents the best case scenario, figure (ii) the worst case scenario.

proposed by Liemberger et al. [11], or after the PSA process. A further feasibility study is required to fully investigate the different possibilities.

It can be concluded that to ensure high purity hydrogen, a pre-layer is required. Without a pre-layer the heavy hydrocarbons will accumulate on the activated carbon and thus reducing the sites available for methane adsorption, resulting in a low purity hydrogen product. Using a pre-layer which is too long, reduces the total amount of activated carbon left and leaving not enough adsorbent to adsorb the methane present in the mixture. The ideal pre-layer therefore has a thickness of 0.2 m, ensuring enough activated carbon present to adsorb all the methane and enough silica gel pre-layer to prevent accumulation of the heavy hydrocarbons.

Techno-economic analysis

In the techno-economic analysis, the use of hydrogen supplied by a PSA system at a hydrogen refuelling station is assessed, in which all costs are calculated using Australian dollars. The cost for compression and storage of the hydrogen required at the station is estimated with the HRSAM model. The initial capital investment costs, which include the installed equipment cost for the compressors, refrigerator, storage tanks, dispenser and the overall control and safety equipment, are to be $6,4 million for medium sized refuelling station with a capacity of 700 kg of H_2/day (see Table 7 in the Supporting Information).

A selective design analysis is performed to estimate the capital investment cost for the PSA, in which only the critical components of the system are analysed. The main components are the adsorbent vessels, the adsorbent material, the valves, and the compressor for compressing the methane off-gas stream back into the pipeline network. The adsorbent material prices, the cost for the pressure vessels, storage tank, and valves are based on quotations of various companies. The compressor cost is calculated using the build in economic analysis tool in Aspen HYSYS. An overview of the equipment cost for the different components is presented in the Supporting Information. The capital investment costs are estimated to be twice the estimated equipment cost, based on previous experiences with building small scale PSA systems.

This results in a total of $1.9 million for the capital investment cost of the designed PSA system.

The costs of the PSA process consists of the maintenance cost of the PSA, the operation cost of the compressor, the capital investment cost spread out over the lifetime of the PSA system, and the feed stock price of the natural gas with 10 vol % hydrogen mixture. The electricity price is varied between 5 and 25 c/kWh. A price range for the natural gas of $9.50/GJ to $15.00/GJ is assumed [26]. It is assumed that the methane rich product stream is supplied back to the gas grid. It must be noted that currently no regulations are in place yet for supplying natural gas back to the grid in Australia.

The best case and worst case scenario for the cost of the PSA are represented in Fig. 8, as a function of the lifetime of the PSA system. The best case scenario assumes an electricity price of 5 c/kWh and a natural gas price of $9.50/GJ, whereas the worst case scenario assumes 25 c/kWh and $15.00/GJ, respectively. Four different centralised hydrogen production methods are considered, which each influence the price of hydrogen which is fed into the natural gas grid. The centralised production of hydrogen through electrolysis is the most expensive method, whereas SMR hydrogen production without CCS is the least expensive [27]. It must be noted that in the calculation, the hydrogen price is calculated as a function of the natural gas price. Therefore, an increased natural gas price results in an increase in the cost price for hydrogen as well. This is not fully representative as hydrogen production costs are expected to decrease, whereas the price for natural gas will increase, but it does provide an insight in the total cost of the PSA system. The influence of the lifetime on the operation cost reduces after 8−10 years for both scenarios.

The final cost price of hydrogen at a refuelling station is compared for three different hydrogen supply methods, as depicted in Fig. 6. This includes the cost for compression, storage, and dispensing (CS&D). In Case A, the hydrogen is supplied by the proposed PSA system. A PSA lifetime of 10 years is assumed, to match the analysis period used in the HRSAM model to calculate the cost for CS&D. A sensitivity analysis on the electricity price (5-25c/kWh) and natural gas price ($9.50−15.00/GJ) is performed. A breakdown of the hydrogen cost price, supplied by a PSA system, is depicted in Fig. 9. Fig. 9 (i) represents the best case scenario, assuming an
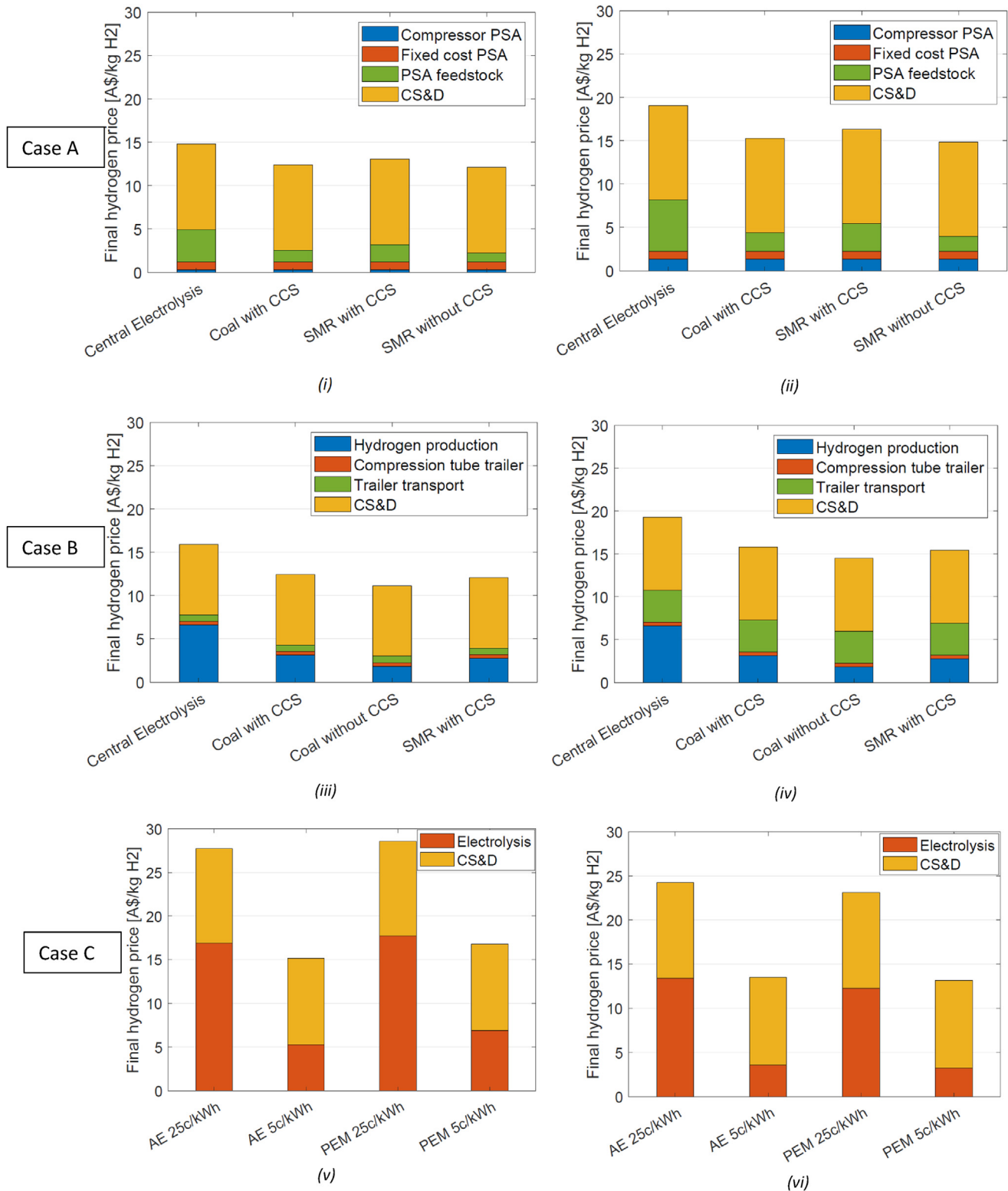
Fig. 9 — Cost break-down for the different hydrogen supply methods analysed. (i) Best case and (ii) worst case scenario for PSA supplied hydrogen at refuelling station. (iii) Best case and (iv) worst case scenario for tube-trailer delivered hydrogen at refuelling station. (v) Current and (vi) future prospected hydrogen price for onsite electrolysis at a refuelling station.

electricity price of 5 c/kWh and a natural gas price of $9.50/GJ, and Fig. 9(ii) the worst case scenario, assuming an electricity price of 25 c/kWh and a natural gas price of $15.00/GJ. In all cases, the CS&D is the major cost component in the final

hydrogen price. The electricity price has a dominant influence on the compressor used to compress the methane rich stream back into the pipeline. Just a slight increase in the cost for the compression, storage, and dispensing is observed. In the best

case scenario, the final hydrogen cost price for green hydrogen (originating from central electrolysis) is $14.79, which can be reduced to $12.14 when grey hydrogen is supplied (originating from SMR without CCS).

In case B, a refuelling station where centralised hydrogen is transported over the road by a tube-trailer as compressed gas is considered. A compression of 350 bar is assumed, with the cost for compression from 35 to 350 bar estimated at $0.42 per kg hydrogen [27]. The influence of the distance travelled by the tube-trailer is analysed, varying from 200 to 1000 km travelled. The cost for transportation are estimated at $2.98 per travelled km [27].

Furthermore, the influence of the electricity price is analysed, varying between 5c/kWh and 25c/kWh. This will influence the CS&D only. The HRSAM model is used to estimate the CS&D cost for a refuelling station where tube-trailer is supplied with hydrogen at a pressure of 350 bar. It must be noted that the cost price for hydrogen produced through electrolysis is fixed at $6.60 for this analysis, as this is the currently estimated price in Australia [27]. The influence of the electricity price was evaluated in case C. As case B focuses on the transport of hydrogen, the influence of the electricity price on the hydrogen cost price produced by electrolysis is not considered.

In Fig. 9 (iii), the best case scenario for tube-trailer transported hydrogen over a distance of 200 km is depicted for different hydrogen production methods, assuming an electricity price of 5c/kWh. The CS&D dominates the final hydrogen price for all four results. If hydrogen produced through coal gasification without CCS is used, the final hydrogen price is lowest, which is as expected. Fig. 9 (iv) represents the worst case scenario, in which a total distance of 1000 km is assumed and an electricity price of 25c/kWh.

To compare the hydrogen price for Case A and Case B, a break-even distance is calculated and tabulated in Table 5. This is calculated for the best case and worst case scenarios, resulting in a break-even distance travelled by the tube-trailer for which the final hydrogen price is equal. The final hydrogen price for transported hydrogen made by electrolysis, will always be more expensive than PSA separated hydrogen with hydrogen originating from central electrolysis in the best case scenario. For hydrogen produced through coal gasification with CCS, the break-even distance is lowest, namely 190 km only. After 190 km travelled by the tube-trailer, the final hydrogen price will always be more expensive than using a PSA at the refuelling station to separate the hydrogen from the natural gas. Thus, with decreasing hydrogen production cost, the break-even distance of the tube-trailer increases. In the worst case scenario of the PSA where hydrogen originates

from central electrolysis, the break-even distance is 940 km. Again, this increases further when the cost for the hydrogen production method decreases.

The last case considered is case C, where the production of hydrogen on-site through electrolysis is examined. This significantly reduces the number of steps to be taken before the hydrogen can be dispensed into the car, as no transport of hydrogen is required. An electrolyser can be connected to the electricity grid, providing a continuous supply of electricity, or it can be connected to a direct renewable energy source such as solar PV or wind. This will reduce the capacity factor and thus increases the cost of the hydrogen produced. According to the National Hydrogen Roadmap, published by Bruce et al. [27], currently the hydrogen price in Australia made from grid connected electricity is around $6.60/kg and $11/kg for hydrogen produced from direct renewables. A capacity factor of 85% is considered for a grid connected electrolyser, whereas for direct renewables a capacity factor of only 35% can be assumed.

In Fig. 9 (v) and (vi) a breakdown of the final hydrogen price for Proton Exchange Membrane (PEM) and Alkaline Electrolyser (AE) cells, for an electricity price of 5c/kWh and 25c/kWh, is depicted. The cost for CS&D is equal to the cost calculated in case A, and again makes up a large part of the final cost price. For an electricity price of 25c/kWh the final hydrogen price is very expensive, even when considering that the cost for the electrolyser is prospected to decrease in 2025. For 5c/kWh electricity price, currently hydrogen can be produced for $15.14. Comparing this to the hydrogen cost price in Case A for hydrogen produced by central electrolysis, which was estimated to be $14.97, the hydrogen price is very comparable. Considering the development of electrolysers in the future, the cost of hydrogen produced on-site by an electrolyser will be less expensive than for a refuelling station of Case A.

However, if the hydrogen is produced as blue or grey hydrogen in Case A, the final hydrogen price will be significantly lower than in Case C. The prospected hydrogen price in 2025 for electrolysers will be slightly above the estimated hydrogen price in the best case scenario for fossil fuel based hydrogen separated by a PSA system in Case A. It is therefore concluded that on-site hydrogen production by electrolysis is strongly influenced by the electricity price and the development of the electrolyser cells will influence the cost estimates for the future.

Conclusion

The designed PSA system shows a promising technical feasibility to produce a high purity hydrogen product and economically feasibility to implement at a hydrogen refuelling station. An optimum PSA separation has been achieved with a 6 bed PSA system, where each column contains a pre-layer of silica gel for the adsorption of heavy hydrocarbons and CO_2, a main layer of activated carbon for methane adsorption, and a post-layer of zeolite LiLSX for nitrogen adsorption. The ideal pre-layer thickness is analysed to be 0.2 m for a column of 1.2 m total height. With this design, hydrogen supplied by a PSA system is economically feasible at a refuelling station. The final hydrogen price, after dispensing, is dominated by the

Table 5 – Break-even distance with hydrogen cost price compared to hydrogen delivered by PSA, for best and worst case scenarios.

	Electrolysis	Coal with CCS	SMR with CCS
Break-even distance (best case) [km]	–	190	470
Break-even distance (worst case) [km]	940	860	1240

cost for compression and storage. Compared to hydrogen supplied by on-site electrolysis, PSA supplied hydrogen is currently a more economical option. On-site electrolysis can become a more economical option in the future with improved cell efficiencies and reduced electricity prices. Tube-trailer transported hydrogen is highly influenced by the distance travelled. If the hydrogen originates from electrolysis, tube-trailer transported hydrogen will always be more expensive. For different fossil fuel based hydrogen technologies, a break-even distance has been calculated. The results of this initial study will help the design of hydrogen transportation and distribution processes in the era of a hydrogen economy. Future work will include experimental validation of the model and further optimisation of the PSA process simulation.

Declaration of competing interest

The authors declare that they have no known competing financial interests or personal relationships that could have appeared to influence the work reported in this paper.

Acknowledgement

Appendix A. Supplementary data

Supplementary data to this article can be found online at https://doi.org/10.1016/j.ijhydene.2022.08.175.

REFERENCES

[1] Emissions Transport. Driving down car pollution in cities. 2016.

[2] COAG Energy Council Hydrogen Working Group. Australia's national hydrogen strategy. Commonwealth of Australia; 2019. https://doi.org/10.1016/s0360-3199(96)90074-9.

[3] Ahmed A, Al-Amin AQ, Ambrose AF, Saidur R. Hydrogen fuel and transport system: a sustainable and environmental future. Int J Hydrogen Energy 2016;41:1369–80. https://doi.org/10.1016/j.ijhydene.2015.11.084.

[4] da Silva Veras T, Mozer TS, da Costa Rubim Messeder dos Santos D, da Silva César A. Hydrogen: trends, production and characterization of the main process worldwide. Int J Hydrogen Energy 2017;42:2018. https://doi.org/10.1016/j.ijhydene.2016.08.219. –33.

[5] Walker SB, Mukherjee U, Fowler M, Elkamel A. Benchmarking and selection of Power-to-Gas utilizing electrolytic hydrogen as an energy storage alternative. Int J Hydrogen Energy 2016;41:7717–31. https://doi.org/10.1016/j.ijhydene.2015.09.008.

[6] Gerboni R. Introduction to hydrogen transportation. Compend Hydrogen Energy 2016:283–99. https://doi.org/10.1016/b978-1-78242-362-1.00011-0. Elsevier Ltd.

[7] Zhang F, Zhao P, Niu M, Maddy J. The survey of key technologies in hydrogen energy storage. Int J Hydrogen Energy 2016;41:14535–52. https://doi.org/10.1016/j.ijhydene.2016.05.293.

[8] Engineering GPA. Hydrogen in the gas distribution networks. 2019.

[9] Murugan A, de Huu M, Bacquart T, van Wijk J, Arrhenius K, te Ronde I, et al. Measurement challenges for hydrogen vehicles. Int J Hydrogen Energy 2019;44:19326–33. https://doi.org/10.1016/j.ijhydene.2019.03.190.

[10] Nikolic DD, Kikkinides ES. Modelling and optimization of hybrid PSA/membrane separation processes. 2015. p. 283–305. https://doi.org/10.1007/s10450-015-9670-z.

[11] Liemberger W, Groß M, Miltner M, Harasek M. Experimental analysis of membrane and pressure swing adsorption (PSA) for the hydrogen separation from natural gas. J Clean Prod 2017;167:896–907. https://doi.org/10.1016/j.jclepro.2017.08.012.

[12] Liemberger W, Halmschlager D, Miltner M, Harasek M. Efficient extraction of hydrogen transported as co-stream in the natural gas grid – the importance of process design. Appl Energy 2019;233–234:747–63. https://doi.org/10.1016/j.apenergy.2018.10.047.

[13] Choi BU, Choi DK, Lee YW, Lee BK, Kim SH. Adsorption equilibria of methane, ethane, ethylene, nitrogen, and hydrogen onto activated carbon. J Chem Eng Data 2003;48:603–7. https://doi.org/10.1021/je020161d.

[14] Rother J, Fieback T. Multicomponent adsorption measurements on activated carbon, zeolite molecular sieve and metal-organic framework. Adsorption 2013;19:1065–74. https://doi.org/10.1007/s10450-013-9527-2.

[15] Mofarahi M, Sadrameli M, Towfighi J. Characterization of activated carbon by propane and propylene adsorption. J Chem Eng Data 2003;48:1256–61. https://doi.org/10.1021/je0340553.

[16] Mayfield PLJ, Do DD. Measurement of the single component adsorption kinetics of ethane , butane , and pentane onto activated carbon using a differential adsorption. Bedrijfskunde 1991:1262–70.

[17] Sircar S, Golden TC. Purification of hydrogen by pressure swing adsorption. Separ Sci Technol 2000;35:667–87. https://doi.org/10.1081/SS-100100183.

[18] Olivier MG, Jadot R. Adsorption of light hydrocarbons and carbon dioxide on silica gel. J Chem Eng Data 1997;42:230–3. https://doi.org/10.1021/je960200j.

[19] Tian C, Fu Q, Ding Z, Han Z, Zhang D. Experiment and simulation study of a dual-reflux pressure swing adsorption process for separating N2/O2. Separ Purif Technol 2017;189:54–65. https://doi.org/10.1016/j.seppur.2017.06.041.

[20] Epiepang FE, Li J, Liu Y, Yang RT. Low-pressure performance evaluation of CO2, H2O and CH4 on Li-LSX as a superior adsorbent for air prepurification. Chem Eng Sci 2016;147:100–8. https://doi.org/10.1016/j.ces.2016.03.022.

[21] Todd RS, He J, Webley PA, Beh C, Wilson S, Lloyd MA. Fast finite-volume method for PSA/VSA cycle simulations - experimental Validation. 2001. p. 3217. https://doi.org/10.1021/ie0008070.

[22] Todd RS, Webley PA. Limitations of the LDF/equimolar counterdiffusion assumption for mass transport within porous adsorbent pellets 2002;57:4227–42.

[23] Bush B, Muratori M, Hunter C, Zuboy J, Melaina M, Bush B, et al. Scenario evaluation and regionalization analysis (SERA) model: demand side and refueling infrastructure buildout. 2019.

[24] Reddi K, Elgowainy A, Sutherland E. Hydrogen refueling station compression and storage optimization with tube-trailer deliveries. Int J Hydrogen Energy 2014;39:19169–81. https://doi.org/10.1016/j.ijhydene.2014.09.099.

[25] Average chemical plant operator hourly pay in Australia. n.d.

[26] Core Energy & Resources Pty Limitedcore. Delivered wholesale gas price outlook 2019-2050. 2019.

[27] Bruce S, Temminghoff M, Hayward J, Schmidt E, Palfreyman D, Hartley P. National hydrogen Roadmap. 2019.